Localization and Segmentation of the Optic Nerve Head in Eye Fundus Images Using Pyramid Representation and Genetic Algorithms

José M. Molina and Enrique J. Carmona

Dpto. de Inteligencia Artificial, ETSI Informática, Universidad Nacional de Educación a Distancia (UNED), Juan del Rosal 16, 28040, Madrid, Spain
jmolina_79@hotmail.com,
ecarmona@dia.uned.es

Abstract. This paper proposes an automatic method to locate and segment the optic nerve head (papilla) from eye fundus color photographic images. The method is inspired in the approach presented in [1]. Here, we use a Gaussian pyramid representation of the input image to obtain a subwindow centered at a point of the papillary area. Then, we apply a Laplacian pyramid to this image subwindow and we obtain a set of interest points (IPs) in two pyramid levels. Finally, a two-phase genetic algorithm is used in each pyramid level to find an ellipse containing the maximum number of IPs in an offset of its perimeter and, in this way, to achieve a progressive solution to the ONH contour. The method is tested in an eye fundus image database and, in relation to the method described in [1], the proposed method provides a slightly lower performance but it simplifies the methodology used to obtain the set of IPs and also reduces the computational cost of the whole process.

1 Introduction

The location and segmentation of the optic nerve head (ONH) is of critical importance in retinal image analysis. The ONH, also called optic disk or papilla, is oval-shaped and is located in the area where all the retina nerve fibres come together to form the start of the optic nerve that leaves the back of the eyeball. There is an area without any nerve fibres called excavation (the centre of the papilla) and around it another area can be found, the neuroretinal ring, whose external perimeter delimits the papillary contour.

Support systems for the diagnosis of eye diseases based on eye fundus image information involve semi-automatic and automatic locating of the papillary contour. Specifically, the first semi-automatic strategies were based on geometric properties of the image pixels and their intensity level values [2].

Active contour-based strategies have also shown to be useful to address this problem. A characteristic property of this type of technique is that it is highly dependent on a preliminary stage of contour initialization, from which the final solution is refined. In some studies, this initialization stage has been done manually, [3,4], and in other instances automatically [5,6].

J.M. Ferrández et al. (Eds.): IWINAC 2011, Part I, LNCS 6686, pp. 431–440, 2011.

Genetic algorithms (GA) have also been used efficiently as a search method to identify the papillary contour [1,7]. Other recent approaches have used different types of techniques like, for example, mathematical morphology [8], image filters [9] or the Hough Transform [10].

Basically, our method uses a Laplacian pyramid of the eye fundus image to obtain a set of interest points (IPs) in each pyramid level. Then a two-phase genetic algorithm is used to achieve a progressive solution to the ONH contour. The method here presented is a variation of the method described in [1]. The main difference between both methods lies in how to get the set of IPs. On the one hand, in the proposed method, the IPs are obtained using a Laplacian pyramid. On the other hand, in [1], they are obtained using a domain-knowledge-based method.

The article is organized as follows: Section 2 describes the methodology of the proposed method. In section 3, the obtained results are evaluated and compared with other methods. Finally, section 4 presents the conclusions and future work.

2 Method Description

The aim of this work is to locate and segment the ONH in eye fundus color photographs through the process shows in the block diagram of the figure 1. First, in order to reduce the processing computational cost, the process begins by automatically extracting a subwindow from the original image. This subwindow is approximately centered at a point of the papillary area. Then a Laplacian pyramid is applied to this image subwindow and the result is an image multi-scale representation where, in each pyramid level, a set of IPs is obtained. These IPs correspond to image points of high-medium frequency, i.e., border points. We use a two-phase GA: GA2+GA1. In both phases, the goal is to search for an ellipse containing the maximum number of IPs in an offset of its perimeter. GA-2 is applied to IPs from level-2 and GA-1 is applied to ones belonging to level 1. GA-2 is run first and, when it completes its execution, the best solutions obtained are used as part of the GA-1 initial population. Finally, after running GA-1, we select the best papillary contour from the final population as the solution of our problem.

2.1 Extracting Subwindow by Gaussian Pyramid

The figure 2 shows the operator block diagram used for extracting an image subwindow from the eye fundus original image, in order to reduce the noise (distracting structures) and the processing computational cost. This operator starts applying a Gaussian pyramid of N-levels to the original image (600x400 pixels). The idea is to smooth the image intensity levels in order to eliminate the image high frequencies. In each pyramid level, the intensity of pixels belonging to the retina, blood vessels and papilla are smoothed in different intensity intervals. The smoothing process is more pronounced as the pyramid level increases. At level-N, the region of the brightest pixels (RBP) will correspond to pixels belonging to the papilla. Here we use the property that the papilla pixels have an

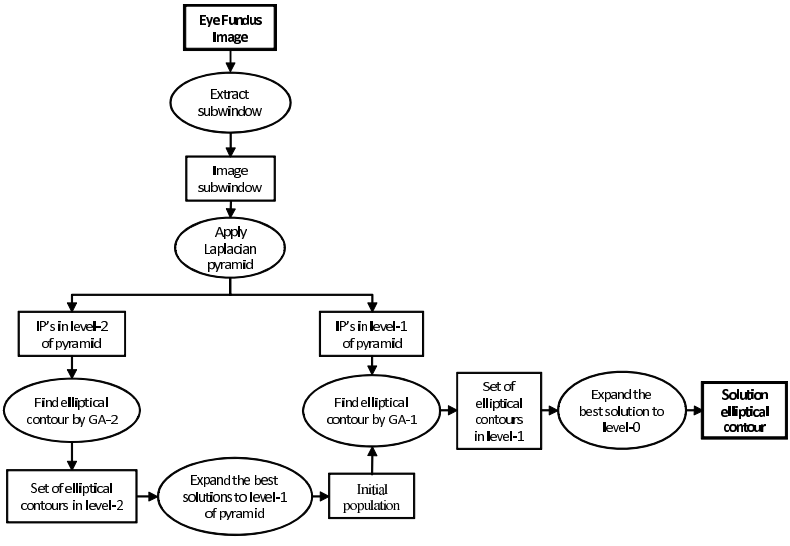

Fig. 1. Method block diagram summarizing the whole process

intensity level higher than retina and blood vessels. Next we invert the process and calculate the inverse pyramid (containing the RBP) up to the level-0 (original image size). At level-0, the centroid of the RBP is calculated and, finally, this centroid is used as central point to built the image subwindow (261x261 pixels). A similar idea is used in [11], where the pyramid is created using a simple Haar-based discrete wavelet transform. Equally, in [12], a first approximation to the pixels detection belonging to the papillary area is done by applying a threshold in each of the three RGB channels. Experimentally, the search for points belonging to the papillary area by this operator on the DRIONS database [13] has produced a 100% success. The Gaussian pyramid only was applied to the image red channel and the number of levels used was N=3. The figure 3 shows the Gaussian pyramid of an input eye fundus image, the inverse Gaussian pyramid (containing RBP) and the final subwindow.

2.2 Obtaining Interest Points by Laplacian Pyramid

The Laplacian pyramid was initially introduced by Burt&Adelson [14] in the context of compression of images. However, this technology has proved be useful in different image analysis tasks: generation and reconstruction, progressive transmission, multi-scale feature detection and enhancement. Just as we may view the Gaussian pyramid as a set of lowpass filtered copies of the original image, we may view the Laplacian pyramid as a set of bandpass filtered copies of the image. The scale of the Laplacian operator doubles from level to level of the pyramid, while the center frequency of the passband is reduced by an octave.

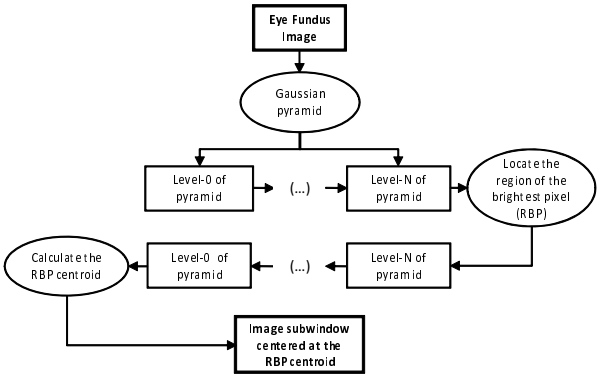

Fig. 2. Diagram summarizing the image subwindow extraction subtask

Thus, the Laplacian pyramid allows a representation of the original image into a hierarchy of images in such a way that each level corresponds to a different band of frequencies.

The characterization of an IP is based mainly on a property by which a point of the image which belongs to the papillary contour presents a change in its intensity level in relation to its neighboring pixels. Nevertheless, this property represents a necessary but not sufficient condition, since there may be other causes that give rise to the appearance of noise associated to other type of intensity level changes. This noise may be due, for instance, to the non-uniform color of the retina or to the existence of blood vessels. In order to reduce the image channel number, we make a weighted sum of the three RGB channels to produce a single image. Then we select as IPs the brightest pixels in the two first levels of the Laplacian pyramid applied to this average image. The figure 4 shows an example of the IPs obtained in each of one of these pyramid levels.

2.3 Obtaining Papillary Elliptic Contours by Genetic Algorithms

Genetic algorithms are one of the paradigms most frequently used in evolutionary computation and they owe their inspiration to the biological process of evolution: natural selection and survival of the fittest individuals [16]. Thus, given a problem of a specific domain, these algorithms code potential solutions using a structure of data like a chromosome (individual) where the genes are parameters of the problem proposed. The approach to the solution of each chromosome is calculated using a fitness function. Finally, by applying selection and variation operators (mutation and recombination), a population of chromosomes evolves to the optimum solution until a finalization criterion is achieved.

Since the human papillary contour is oval-shaped, this work proposes searching for the solution by approaching this contour with an ellipse, like is done in other works, e.g. [1,6,15]. From this instant, it is assumed that: (1) the geometric shape of the papilla can be approached by a non-deformable ellipse, and (2) the

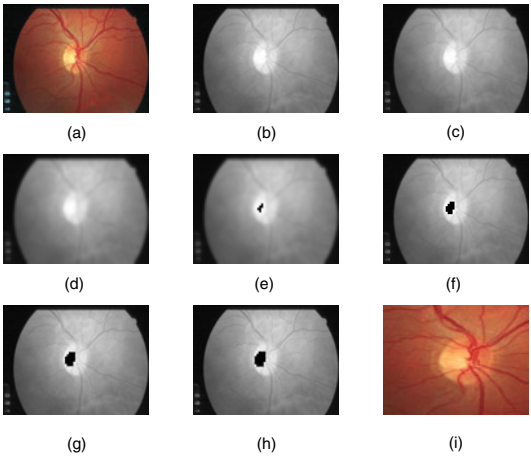

Fig. 3. An example that shows the different phases of the image subwindow extraction task: (a) original image at level 0; (b-d) image red channel Gaussian pyramid, showing levels 1, 2 and 3, respectively; (e) region of the brightest points (RBP) in level 3, represented by the centered black pixels; (f-h) inverse Gaussian pyramid (containing RBP): levels 2, 1 and 0, respectively; (i) final image subwindow centered at level-0 RMP centroid

more IPs that the ellipse contains, the more likely this ellipse will approach the real contour of the papilla. The results obtained in [1] support the validity of the two hypotheses.

Specifically, we use a two-phase GA: GA-2+GA-1 (see figure 1). GA-2 is applied to level-2 of pyramid to find an ellipse containing the maximum number of IPs in an offset of its perimeter. The result is a first approximation to our problem, i.e., a set of papillary contours in that level. Now, we expand the best contours obtained previously from level-2 to level-1 for using them as part of the GA-1 initial population. The other subset of individuals, needed to complete the GA-1 initial population, is obtained randomly. Then GA-1 is applied to IPs of level-1 with the same goal than GA-2. Finally, in order to produce the solution, the best papillary contour obtained by GA-1 is expanded from level-1 to image subwindow original level (level-0). At this point, it is important to say that we do not work in the Laplacian pyramid level-0 because the IPs obtained in this level contain a lot of noise.

The phenotypic space, solution space of the original problem, consists of the elliptic crown space defined from the infinite ellipses that can be traced in the image. To code this type of solutions, the phenotypic space is transformed into a genotypic space consisting of real vectors of five variables $[x, y, a, b, \omega]$. Thus, (x, y) represents the centre of this ellipse, (a, b) the magnitudes of its major and minor semi-axis respectively and ω the angle that its major axis forms with the x-axis. The fitness function is defined by counting the IPs number confined

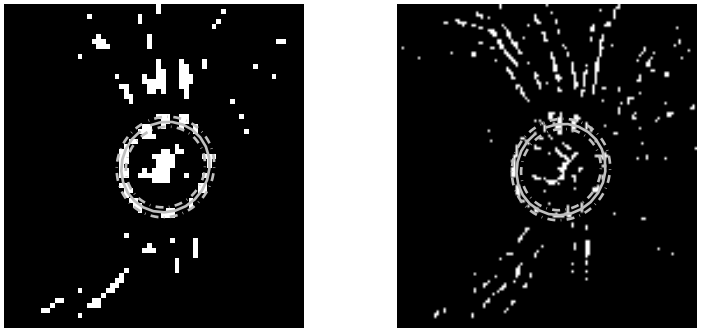

Fig. 4. Examples of sets of IPs and papillary genetic ellipses obtained: (a) Laplacian pyramid level-2; (b) Laplacian pyramid level-1. Genetic ellipses (solid lines), elliptical crowns (dashed lines)

within a concentric elliptical crown that contains the genetic ellipse. Figure 4 shows two solution ellipses adapted to the set of IPs obtained in the two levels of Laplacian pyramid: level 2 (Fig. 4a) and level 1 (Fig. 4b).

The table 1 summarizes the domain of definition of each gene used in the executions of GA-1 and GA-2. These values are obtained from [1], but they are transformed taking in count the image resolution in the pyramid levels 1 and 2. Finally, the table 2 summarizes the configuration values of each of the two AGs used in our approach.

Table 1. Definition domain (expressed in pixels) for each of the genes (variables) of a chromosome (genetic ellipse)

	GA-2	GA-1
Image Size	65x65	129x129
$[x_{min},\ x_{max}]$	[15, 50]	[30, 100]
$[y_{min},\ y_{max}]$	[15, 50]	[30, 100]
$[a_{min},\ a_{max}]$	[8, 15]	[16, 30]
$[b_{min},\ b_{max}]$	[8, 15]	[16, 30]
$[\omega_{min},\ \omega_{max}]$	[15°, 175°]	[15°, 175°]

3 Experiments and Results

To measure the performance of our algorithm, we used DRIONS database [13]. In order to do the result of the evaluation quantitatively reproducible, we measured the mean discrepancy between the points of the contour obtained with the segmentation method and a gold standard defined from a contour that was the result of averaging two contours, each of them traced by an expert. Here we use

Table 2. Summary of the configuration of the two AGs used in our approach

AG Parameter	GA-2	GA-1
Initialisation	Random	Random and best solutions of GA-1
Representation	Real vector (dim: 1 X 5)	
Recombination	One-point crossover	
Mutation	Non-uniform with Gaussian distribution	
Parent selection	Stochastic uniform	
Survival selection	Generational without elite	Generational with elite

the concept of discrepancy, δ, defined in [1,6]. For visualization purposes, the ogive of discrepancy is plotted, namely, the percentage of images with discrepancy less than δ (y-axis) versus δ (x-axis).

3.1 Experiment Results

Different experiments were done in order to choose the best values related to the intrinsic parameters of our two-phase GA: population size (P), number of generations (G), elite population size (E), crossover ratio (C) and shrink value (S). The latter controls the ratio with which the mean mutation magnitude decreases and it is related to the non-uniform mutation operator with Gaussian distribution applied with a probability of one per gene. In the light of the results obtained in the experiments, the following final parameter configuration was chosen: P2=200, G2=20, C2=0.2, S2=0.8, E2=0 (for GA-2,) and P1=100, G1=50, C1=0.2, S1=0.8, E1=1 (for GA-1). The GA-1 initial population was created using 50% best solutions of the GA-2. The rest of the GA1 initial population was randomly obtained. In order to achieve a competitive result, we searched for a compromise between quality of results and computational cost.

3.2 Evaluation and Comparison of Results

In the bibliography consulted by the authors related to ONH segmentation from eye fundus color images and discarding the evaluations done subjectively and not quantitatively, we believe that the Lowell's [6] and Carmona's [1] methods are the ones that have obtained better results. Therefore, we will use these approaches as reference. Thus figure 5 shows the discrepancy curves obtained from applying the three methods to DRIONS database [13]. Specifically, the Lowell's and Carmona's curves were obtained directly from [1]. On the other hand, owing to the stochastic nature associated with the GA, the curve of discrepancy obtained by our method corresponds to the result of averaging five of them obtained as a result of executing our two-phase GA five times.

Direct comparison of the discrepancy curve obtained by Lowell's method and our method reveals two very different areas with opposite behavior, whose boundary is marked by the value $\delta = 1.4$. Below this value, Lowell's results are slightly better than our proposal, and above this value, precisely the opposite

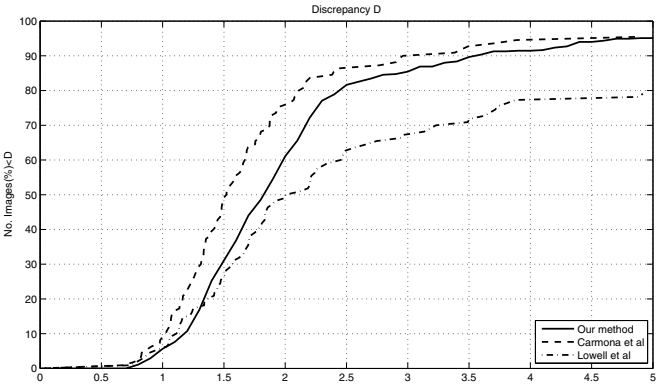

Fig. 5. Accumulated discrepancy results for our segmentaation method versus Carmona et al [1]and Lowell et al [6]

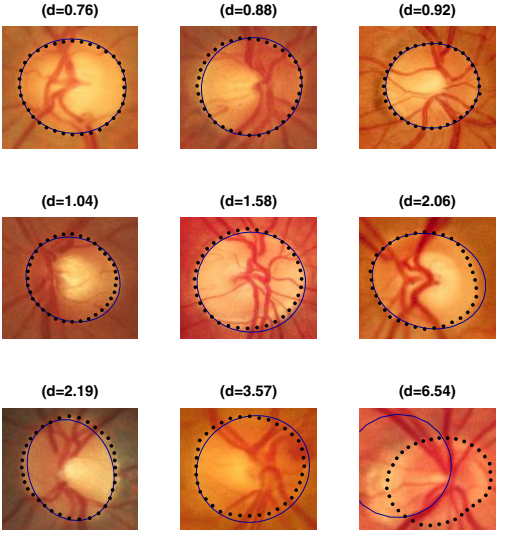

Fig. 6. Several examples of segmentation obtained with our method (solid line). The gold standard is represented by dotted line.

occurs. We think that the explanation for the results obtained in the first discrepancy subinterval $(0, 1.4)$ is that while our method approaches the solution using a non deformable ellipse, the local deformation phase in Lowell's method makes it possible to do a slight deformation of the ellipse, obtaining a better approaches the experts' real trace. However, the change in trend on the second subinterval $(1.4, 5)$ reveals the robustness of our method. In fact, while Lowell's method only obtains 80% of images below a discrepancy $\delta = 5$, our method obtains 95%.

The comparison of the discrepancy curve obtained by Carmona's method reveals that our method has a behavior slightly worse in all the discrepancy range. The explanation of this behavior could be due to the fact that the final genetic contour of our method is obtained in the Laplacian pyramid level-1, i.e, we need to expand that solution to the original image level. This fact could also explain why the gap between both discrepancy curves is more pronounced for low levels of discrepancy and less pronounced for high values. In fact, for a discrepancy value of $\delta = 5$, both methods match their performance. On the other hand, the computational cost of our method is lower: 9.000 evaluations of the fitness function against 20.000 evaluations used by Carmona's method.

Finally, the figure 6 shows different examples of papillary contours obtained in this work and they are compared with the experts' gold standard.

4 Conclusions and Future Work

We have described a new automatic method to locate and segment the ONH in eye fundus color photographic images. This method is inspired in the approach presented in [1]. The performance of our method was compared with two competitive methods in the literature.

In relation to the results obtained in [1], we obtain a slightly lower performance. In contrast, our method has shown to be faster. Also, the way of obtaining our set of IPs is simpler: our fitness function only pays attention to the number of IPs inside the elliptic crown, i.e., it is independent of the domain knowledge. Finally, we can also say that our method outperforms the results obtained by [6] in most of the discrepancy domain ($\delta > 1.4$).

A disadvantage of our method is that we cannot work at Laplacian pyramid level-0 because the set of IPs obtained in that level contains a lot of noise. Therefore, we have to expand directly the genetic solution obtained from level-1 to level-0, but this operation seems to produce a lack of accuracy. We propose as future work to investigate other types of multi-resolution image representation techniques like wavelet transform or apply images filter directly in the input image (level-0) in order to obtain sets of IPs with a low level of noise.

Acknowledgment. This work was supported in part by funds of the Advanced Artificial Intelligence Master Program of the Universidad Nacional de Educación a Distancia (UNED), Madrid, Spain.

References

1. Carmona, E.J., Rincón, M., García-Feijoo, J., Martínez-de-la-Casa, J.M.: Identification of the Optic Nerve Head with Genetic Algorithms. Artificial Intelligence in Medicine 43(3), 243–259 (2008)
2. Cox, J., Wood, I.: Computer-assisted optic nerve head assessment. Ophthalmic and Physiological Optic 11(1), 27–35 (1991)

3. Morris, T., Donnison, C.: Identifying the neuroretinal rim boundary using dynamic contours. Image and Vision Computing 17(3-4), 169–174 (1999)
4. Mendels, F., Heneghan, C., Thiran, J.: Identification of the optic disk boundary in retinal images using active contours. In: Proceedings of the Irish Machine Vision and Image Processing Conference (IMVIP 1999), pp. 103–115 (1999)
5. Osareh, A., Mirmehdi, M., Thomas, B., Markham, R.: Colour morphology and snakes for optic disc localisation. In: Proceedings of the 6th Medical Image Understanding and Analysis Conference, pp. 21–24 (2002)
6. Lowell, J., Hunter, A., Steel, D., Basu, A., Ryder, R., Fletcher, E., Kennedy, L.: Optic nerve head segmentation. IEEE Transaction on Medical Imaging 23(2), 256–264 (2004)
7. Novo, J., Penedo, M.G., Santos, J.: Localisation of the optic disc by means of GA-optimised Topological Active Nets. Image and Vision Computing 27(10), 1572–1584 (2009)
8. Welfer, D., Scharcanski, J., Kitamura, C.M., Dal Pizzol, M.M., Ludwig, L.W.B., Ruschel, D.: Segmentation of the optic disk in color eye fundus images using an adaptive morphological approach. Computers in Biology and Medicine 40, 124–137 (2010)
9. Rangayyan, R.M., Zhu, X., Ayres, F.J., Ells, A.L.: Detection of the Optic Nerve Head in Fundus Images of the Retina with Gabor Filters and Phase Portrait Analysis. Journal of Digital Imaging 23(4), 438–453 (2010)
10. Zhu, X., Rangayyan, R.M., Ells, A.L.: Detection of the Optic Nerve Head in Fundus Images of the Retina Using the Hough Transform for Circles. Journal of Digital Imaging 23(3), 332–341 (2010)
11. Lalonde, M., Beaulieu, M., Gagnon, L.: Fast and Robust Optic Disc Detection Using Pyramidal Decomposition and Hausdorff-Based Template Matching. IEEE Transactions on Medical Imaging 20(11), 1193–1200 (2001)
12. Bachiller, M., Rincón, M., Mira, J., García-Feijó, J.: An automatic system for the location of the optic nerve head from 2D images. In: Mira, J., Prieto, A.G. (eds.) IWANN 2001. LNCS, vol. 2085, pp. 319–327. Springer, Heidelberg (2001)
13. DRIONS-DB: Digital Retinal Images for Optic Nerve Segmentation Database, `http://www.ia.uned.es/personal/ejcarmona/DRIONS-DB.html` (accessed on August 21, 2009)
14. Burt, P.J., Adelson, E.H.: The Laplacian Pyramid as a Compact Image Code. IEEE Transactions on Communications 31(4), 532–540 (1983)
15. Shields, M.B.: Color atlas of glaucoma. Williams and Wilkins, Baltimore (1998)
16. Holland, J.H.: Adaption in Natural and Artificial Systems. MIT Press, Cambridge (1992)